NUMERICAL ANALYSIS OF UNSTEADY MOTION OF A RAREFIED GAS CAUSED BY SUDDEN CHANGE OF WALL TEMPERATURE WITH SPECIAL INTEREST IN THE PROPAGATION OF DISCONTINUITY IN THE VELOCITY DISTRIBUTION FUNCTION(Mathematical Analysis of Phenomena in Fluid and Plasma Dynamics)

AUTHOR(S):

Aoki, Kazuo; Sone, Yoshio; Nishino, Kenji; Sugimoto, Hiroshi

数理解析研究所講究録
第745巻 1991年 232-241

NUMERICAL ANALYSIS OF UNSTEADY MOTION OF A RAREFIED GAS CAUSED BY SUDDEN CHANGE OF WALL TEMPERATURE WITH SPECIAL INTEREST IN THE PROPAGATION OF DISCONTINUITY IN THE VELOCITY DISTRIBUTION FUNCTION

Kazuo Aoki, Yoshio Sone, Kenji Nishino, and Hiroshi Sugimoto
（青木一生，　曾根良夫，　西野健司，　杉元宏）

Department of Aeronautical Engineering, Kyoto University, Kyoto 606, Japan
（京大・工・航空）

An unsteady gas motion induced in a semi-infinite expanse of a rarefied gas by sudden heating (or cooling) of the plane wall bounding the gas is analyzed numerically on the basis of the Boltzmann-Krook-Welander equation and the diffuse reflection. The time development of the disturbance in the gas is pursued, for various cases of heating and cooling, over a long time from the initial moment when the heating or cooling occurs. In particular, the propagation and attenuation of the discontinuity in the velocity distribution function are analyzed accurately.

I. INTRODUCTION

Consider a semi-infinite expanse of a rarefied gas in a uniform equilibrium state at rest, bounded by a plane solid wall. Provided that the wall temperature changes suddenly, a gas motion is induced owing to expansion or contraction of the gas by heating or cooling and the disturbances propagate into the gas. This simple initial and boundary value problem is of physical interest because it exhibits the fundamental feature of the transition from the free molecular to the continuum behavior of the gas. For a small temperature change, a systematic analysis based on the linearized equation was carried out, and analytical results for short and long time behavior were obtained.[1] For a large temperature change, the problem was studied by a moment method, but the result showed some unphysical behavior.[2]

In the present study, we will carry out an accurate numerical analysis of the problem for arbitrary temperature changes to obtain the behavior of the gas precisely over a long time from the initial moment when the wall temperature changes, with special emphasis on the following point. In the present problem, the velocity distribution function is discontinuous on the wall at the initial moment, and the discontinuity propagates into the gas, decaying owing to molecular collisions. This situation cannot be described correctly by the standard finite-difference method, such as used in Refs. 3-5. In the recent study of unsteady strong evaporation form a plane condensed phase,[6,7] Sone and Sugimoto developed a numerical method (finite-difference method on the characteristic coordinates) describing the discontinuity in the velocity distribution function correctly. On the basis of their idea, we try to construct a more efficient method to capture the behavior of the discontinuity.

II. PROBLEM AND BASIC EQUATION

Problem: Consider a semi-infinite expanse of a rarefied gas ($X_1 > 0$, X_i: rectangular space coordinates) in contact with a stationary plane wall ($X_1 = 0$, temperature T_0) and in a uniform equilibrium state at rest (temperature T_0, pressure p_0). Suppose that the wall temperature changes discontinuously to another uniform temperature T_1 at time $t = 0$ and is kept at T_1 for all $t > 0$. Investigate the unsteady behavior of the gas for $t > 0$ on the basis of the kinetic theory.

We analyze the problem under the following assumptions: (i)The behavior of the gas is described by the Boltzmann-Krook-Welander equation; (ii)The gas molecules are reflected diffusely on the wall.

The Boltzmann-Krook-Welander equation in the present spatially one-dimensional case is written in the following form.

$$\frac{\partial f}{\partial t}+\xi_1\frac{\partial f}{\partial X_1}=A_c\rho(f_e-f), \tag{1}$$

$$f_e=\frac{\rho}{(2\pi RT)^{3/2}}\exp\left(-\frac{(\xi_1-v_1)^2+\xi_2^2+\xi_3^2}{2RT}\right), \tag{2}$$

$$\left.\begin{aligned}&\rho=\int f d\xi_1 d\xi_2 d\xi_3, \qquad v_1=\frac{1}{\rho}\int \xi_1 f d\xi_1 d\xi_2 d\xi_3,\\ &T=\frac{1}{3R\rho}\int[(\xi_1-v_1)^2+\xi_2^2+\xi_3^2]f d\xi_1 d\xi_2 d\xi_3, \qquad p=R\rho T,\end{aligned}\right\} \tag{3}$$

where $f(X_1,t,\xi_i)$ is the velocity distribution function, ξ_i is the molecular velocity, $\rho(X_1,t)$ is the gas density, $v_i(X_1,t)=(v_1(X_1,t),0,0)$ is the gas flow velocity, $T(X_1,t)$ is the gas temperature, $p(X_1,t)$ is the gas pressure, R is the gas constant per unit mass, A_c is a constant ($A_c\rho$ is the collision frequency of the gas molecules), and the domain of integration is the whole space of ξ_i.

The diffuse-reflection boundary condition on the wall is

$$f=\frac{\sigma}{(2\pi RT_1)^{3/2}}\exp\left(-\frac{\xi_i^2}{2RT_1}\right), \qquad \text{for } \xi_1>0, \text{ at } X_1=0, \tag{4}$$

where

$$\sigma=-\left(\frac{2\pi}{RT_1}\right)^{1/2}\int_{\xi_1<0}\xi_1 f(0,t,\xi_i)d\xi_1 d\xi_2 d\xi_3. \tag{5}$$

The boundary condition at infinity and the initial condition are

$$f=\frac{\rho_0}{(2\pi RT_0)^{3/2}}\exp\left(-\frac{\xi_i^2}{2RT_0}\right), \text{ (for } \xi_1<0, \text{ as } X_1\to\infty) \text{ and (for all } \xi_i, \text{ at } t=0), \tag{6}$$

where $\rho_0=p_0(RT_0)^{-1}$ is the gas density at the initial state.

According to Ref. 8, we can reduce the system (1)-(6) to that for g and h defined below, where ξ_2 and ξ_3 are eliminated. That is, with $\Phi(x,\bar{t},\zeta)=[\![g,h]\!]$, the basic equation (1) with (2), (3) is reduced to

$$\frac{\partial\Phi}{\partial\bar{t}}+\zeta\frac{\partial\Phi}{\partial x}=\frac{2}{\sqrt{\pi}}\frac{\rho}{\rho_0}(\Psi-\Phi), \tag{7}$$

$$\Psi(\mathrm{M},\zeta)=\left[\!\!\left[1,\frac{T}{T_0}\right]\!\!\right]\frac{1}{\sqrt{\pi}}\frac{\rho}{\rho_0}\left(\frac{T}{T_0}\right)^{-1/2}\exp\left(-(\zeta-\frac{v_1}{(2RT_0)^{1/2}})^2\left(\frac{T}{T_0}\right)^{-1}\right), \tag{8}$$

$$\left.\begin{aligned}&\mathrm{M}(x,\bar{t})=\left[\!\!\left[\frac{\rho}{\rho_0},\frac{v_1}{(2RT_0)^{1/2}},\frac{T}{T_0}\right]\!\!\right],\\ &\frac{\rho}{\rho_0}=\int_{-\infty}^{\infty}g d\zeta, \qquad \frac{v_1}{(2RT_0)^{1/2}}=\left(\frac{\rho}{\rho_0}\right)^{-1}\int_{-\infty}^{\infty}\zeta g d\zeta,\\ &\frac{T}{T_0}=\frac{2}{3}\left(\frac{\rho}{\rho_0}\right)^{-1}\left\{\int_{-\infty}^{\infty}(\zeta-\frac{v_1}{(2RT_0)^{1/2}})^2 g d\zeta+\int_{-\infty}^{\infty}h d\zeta\right\},\end{aligned}\right\} \tag{9}$$

where

$$\left.\begin{aligned}&g(x,\bar{t},\zeta)=(2RT_0)^{1/2}\rho_0^{-1}\iint_{-\infty}^{\infty}f(X_1,t,\xi_i)d\xi_2 d\xi_3,\\ &h(x,\bar{t},\zeta)=(2RT_0)^{-1/2}\rho_0^{-1}\iint_{-\infty}^{\infty}(\xi_2^2+\xi_3^2)f(X_1,t,\xi_i)d\xi_2 d\xi_3,\\ &x=\ell_0^{-1}X_1, \qquad \bar{t}=t_0^{-1}t, \qquad \zeta=(2RT_0)^{-1/2}\xi_1,\\ &\ell_0=(8RT_0/\pi)^{1/2}(A_c\rho_0)^{-1}, \qquad t_0=(2RT_0)^{-1/2}\ell_0,\end{aligned}\right\} \tag{10}$$

ℓ_0 is the mean free path of the gas molecules at the initial equilibrium state at rest at temperature T_0 and pressure p_0, and t_0 is the corresponding mean free time multiplied by $2/\sqrt{\pi}$. The boundary condition at $X_1 = 0$, (4), is reduced to

$$\Phi = \Psi(\rho = \sigma, v_1 = 0, T = T_1), \qquad \text{for } \zeta > 0, \text{ at } x = 0, \tag{11}$$

$$\frac{\sigma}{\rho_0} = -2\sqrt{\pi}\left(\frac{T_1}{T_0}\right)^{-1/2} \int_{-\infty}^{0} \zeta g(0, \bar{t}, \zeta) d\zeta. \tag{12}$$

The boundary condition at infinity and the initial condition, (6), are reduced to

$$\Phi = \Psi(\rho = \rho_0, v_1 = 0, T = T_0), \qquad (\text{for } \zeta < 0, \text{ as } x \to \infty) \text{ and (for all } \zeta, \text{ at } \bar{t} = 0)\ . \tag{13}$$

We solve this system numerically by a finite-difference method for various values of T_1/T_0, which is the only parameter of the problem.

III. NUMERICAL ANALYSIS

For $\zeta > 0$, the velocity distribution function Φ is discontinuous at $(x, \bar{t}) = (0, 0)$ (point O in Fig. 1.), i.e., $\lim_{\bar{t}\to 0} \Phi(0, \bar{t}, \zeta) \neq \lim_{x\to 0} \Phi(x, 0, \zeta)$, from the initial and boundary data (11), (13). This discontinuity propagates into the gas along each characteristic line $x = \zeta\bar{t}$ of (7), depending on ζ, as time goes on. Therefore, Φ is discontinuous on the surface $x = \zeta\bar{t}$ $(\zeta > 0)$ in the $(x, \bar{t}, \zeta)$ space. On the other hand, Φ is continuous for $\zeta < 0$. The macroscopic variables, M, are continuous in the $(x, \bar{t})$ plane. The discontinuity in Φ is expected to decay rapidly with time (exponentially in $\bar{t}$) owing to molecular collisions.

In Refs. 6, 7, and 9, the characteristic coordinate system is used in describing the above type of discontinuity of the initial stage. Here in order to improve the efficiency of computation we introduce a hybrid system which is basically a standard implicit finite-difference scheme with auxiliary characteristic coordinates.

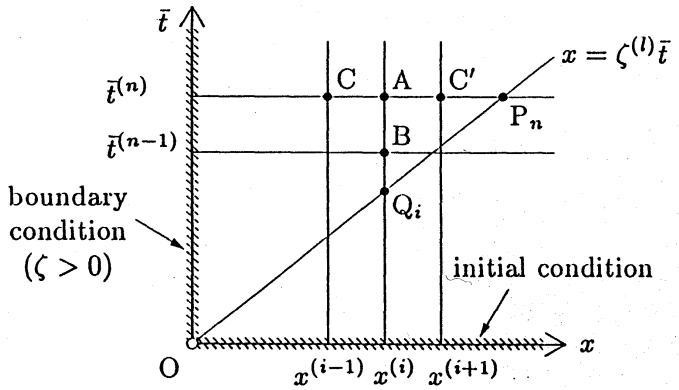

Fig. 1. The $(x, \bar{t})$ plane.

(i)Scheme for the initial stage

Let $(x^{(i)}, \bar{t}^{(n)}, \zeta^{(l)})$ be the lattice points in the $(x, \bar{t}, \zeta)$ space. We take lattice points A: $(x^{(i)}, \bar{t}^{(n)})$, B: $(x^{(i)}, \bar{t}^{(n-1)})$, C: $(x^{(i-1)}, \bar{t}^{(n)})$, C′: $(x^{(i+1)}, \bar{t}^{(n)})$ in the $(x, \bar{t})$ plane and denote the intersection of the characteristic line $x = \zeta^{(l)}\bar{t}$ with $\bar{t} = \bar{t}^{(n)}$ by P_n and that with $x = x^{(i)}$ by Q_i (Fig. 1). For simplicity the set of arguments $(x, \bar{t})$ in Φ and M will be represented by the symbol of the corresponding point, i.e., Φ(A), M(B), etc.

(a)The case where $\zeta^{(l)} > 0$ and the characteristic line $x = \zeta^{(l)}\bar{t}$ does not intersect the segment CAB, or the case where $\zeta^{(l)} < 0$: A standard implicit scheme with first-order accuracy is used. That is, in (7) we replace $\partial\Phi/\partial\bar{t}$ by the finite difference $[\Phi(\mathrm{A}) - \Phi(\mathrm{B})]/(\bar{t}^{(n)} - \bar{t}^{(n-1)})$ and $\partial\Phi/\partial x$

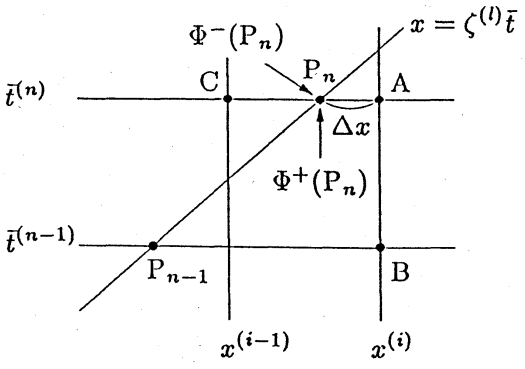

Fig. 2. The case where $x = \zeta^{(l)}\bar{t}$ ($\zeta^{(l)} > 0$) intersects $\overline{CA}$.

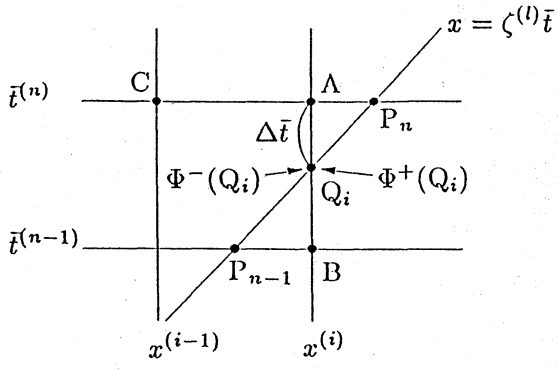

Fig. 3. The case where $x = \zeta^{(l)}\bar{t}$ ($\zeta^{(l)} > 0$) intersects $\overline{AB}$.

by $[\Phi(A) - \Phi(C)]/(x^{(i)} - x^{(i-1)})$ for $\zeta^{(l)} > 0$ or $[\Phi(C') - \Phi(A)]/(x^{(i+1)} - x^{(i)})$ for $\zeta^{(l)} < 0$ and assume that $\Phi = \Phi(A)$, $M = M(B)$ on the right-hand side. Then, $\Phi(A)$ is determined from $\Phi(B)$, $\Phi(C)$, and $M(B)$ for $\zeta^{(l)} > 0$ and from $\Phi(B)$, $\Phi(C')$, and $M(B)$ for $\zeta^{(l)} < 0$.

(b)The case where $x = \zeta^{(l)}\bar{t}$ ($\zeta^{(l)} > 0$) intersects the segment CA (Fig. 2): In scheme (a), the $\partial\Phi/\partial x$ term, $[\Phi(A) - \Phi(C)]/(x^{(i)} - x^{(i-1)})$, is replaced by $[\Phi(A) - \Phi^+(P_n)]/\Delta x$, where $\Delta x = x^{(i)} - \zeta^{(l)}\bar{t}^{(n)}$ and $\Phi^{\pm}(P_n)$ is the limiting value of Φ as $(x, \bar{t}) \to P_n$ with $x \gtrless \zeta^{(l)}\bar{t}$ (the upper or lower signs go together). Then, if $\Phi^+(P_n)$ is known, $\Phi(A)$ is determined from $\Phi^+(P_n)$, $\Phi(B)$, and $M(B)$.

(c)The case where $x = \zeta^{(l)}\bar{t}$ ($\zeta^{(l)} > 0$) intersects the segment AB (Fig. 3): In scheme (a), the $\partial\Phi/\partial\bar{t}$ term, $[\Phi(A) - \Phi(B)]/(\bar{t}^{(n)} - \bar{t}^{(n-1)})$, is replaced by $[\Phi(A) - \Phi^-(Q_i)]/\Delta\bar{t}$, where $\Delta\bar{t} = \bar{t}^{(n)} - (x^{(i)}/\zeta^{(l)})$ and $\Phi^-(Q_i)$ is computed by the linear interpolation from $\Phi^-(P_n)$ and $\Phi^-(P_{n-1})$. Therefore, if $\Phi^-(P_n)$ is known, $\Phi(A)$ is determined from $\Phi(C)$, $\Phi^-(P_n)$, and $M(B)$.

(d)Evaluation of Φ on both sides of the characteristic, $\Phi^+(P_n)$ and $\Phi^-(P_n)$: The Φ at $\bar{t} = \bar{t}^{(n)}$ on both sides of the characteristic line $x = \zeta^{(l)}\bar{t}$, i.e., $\Phi^{\pm}(P_n)$, are obtained from the finite difference equation along the characteristic $x = \zeta^{(l)}\bar{t}$, which are obtained by replacing $(\partial\Phi/\partial\bar{t}) + \zeta(\partial\Phi/\partial x)$ by $[\Phi^{\pm}(P_n) - \Phi^{\pm}(P_{n-1})]/(\bar{t}^{(n)} - \bar{t}^{(n-1)})$, Φ by $\Phi^{\pm}(P_n)$, and M by $M(P_{n-1})$ in (7). The $M(P_{n-1})$ is approximated by the linear interpolation from M at the neighboring lattice points on $\bar{t} = \bar{t}^{(n-1)}$ since M is continuous in x and $\bar{t}$.

Applying the above scheme (a)-(d) to the first time step $\bar{t} = \bar{t}^{(1)}$, we determine Φ at $t = \bar{t}^{(1)}$ from large to small x for $\zeta^{(l)} < 0$ with the aid of the initial condition and the boundary condition at infinity (13) and from small to large x for $\zeta^{(l)} > 0$ with the aid of the initial condition (13) and the boundary condition on the wall (11). We repeat this process to obtain Φ at the subsequent time steps.

(ii)Scheme for subsequent time

After the discontinuity in Φ essentially disappears, we switch the scheme to a standard finite-difference scheme with second-order accuracy [(20a, b) and (22a, b) in Ref. 5 with the time derivative term replaced by the standard finite difference of second-order accuracy (the lattice division is different)], which is more straightforward and is efficient for long-time computation, and continue the computation by the similar process to that of the initial stage.

The appropriate combination of the two different schemes (i) and (ii) makes it possible to evaluate the velocity distribution function accurately at any instant.

IV. RESULT

Finally, we summarize the main result of the numerical analysis.

A. The case of sudden heating ($T_1/T_0 > 1$)

We show the time development of the profiles of the temperature T, pressure p, and flow velocity v_1 for $T_1/T_0 = 2$ in Figs. 4a ($0 \leq t/t_0 \leq 16$), 4b ($10 \leq t/t_0 \leq 100$), and 4c ($100 \leq t/t_0 \leq 10000$), where the scales of the ordinates, common to the three figures, are shown in Fig. 4a. In Table I, we give the corresponding time evolution of the values of the energy flow H_1, normal stress p_{11}, temperature T, and pressure p at the wall, where H_i is the energy flow vector ($H_2 = H_3 = 0$) and p_{ij} is the stress tensor ($p_{12} = p_{13} = p_{23} = 0$) defined, respectively, by

$$H_i = \frac{1}{2}\int \xi_i \xi_j^2 f d\xi_1 d\xi_2 d\xi_3, \qquad p_{ij} = \int (\xi_i - v_i)(\xi_j - v_j) f d\xi_1 d\xi_2 d\xi_3. \tag{14}$$

The pressure rise near the wall by sudden heating pushes the gas away from the wall and sends out a compression wave (shock wave) toward infinity in the gas. Then, the density near the wall begins to decrease because there is no mass injection from the wall to compensate the gas flow. This leads to a pressure decrease since the energy supply from the wall, which decreases with the temperature rise near the wall, is insufficient, and an expansion wave is sent out to run after the shock wave. The expansion wave finally overtakes the shock wave and weakens it. For large t/t_0, the amplitude of the shock wave decreases very slowly, and its propagation speed approaches the sound speed at the equilibrium state at rest with temperature T_0 and pressure p_0. As regards the temperature field, only a small part of the disturbance propagates as the shock wave, and the rest diffuses slowly. The velocity profile behind the shock wave has a shoulder. The region near the wall where the slope of the profile is larger corresponds to the diffusion region. The gas is heated by diffusion and is pushed outward there. The heating and piston effect gets weaker as time goes on. Correspondingly, expansion waves are continuously sent out to accommodate the diffusion region and the region behind the shock wave. Thus, the region between the shoulder and shock wave is the region of expansion waves. Since a wave sent out at later time is weaker, the variation of physical quantities in the expansion wave region is larger farther away from the wall, that is, the variation is largest just behind the shock wave (see Fig. 4c). In the limit of $t/t_0 \to \infty$, the state of the gas approaches the uniform equilibrium state at rest with temperature T_1 and pressure p_0.

For $T_1/T_0 = 2$, the reduced velocity distribution function g at $t/t_0 = 0.5, 2$, and 10 is shown in Fig. 5 as a function of $(2RT_0)^{-1/2}\xi_1$. The discontinuity of g in the gas attenuates rapidly with time due to molecular collisions and is invisible at $t/t_0 = 10$. The discontinuity at the wall decays slowly.

In Fig. 6 and Table I, we give some results for a small temperature rise, i.e., $T_1/T_0 = 1.1$. The feature of the flow field is very similar to that for $T_1/T_0 = 2$ except that the amplitude of the disturbance is small*. In Table I, the analytical results[1] of the temperature and pressure for short time and long time based on the linearized equation, supplemented by more recent and accurate data[10] for the numerical coefficients, are also shown for comparison.

B. The case of sudden cooling ($T_1/T_0 < 1$)

For $T_1/T_0 = 0.5$, we show the time development of the profiles of T, p, and v_1 in Figs. 7a, b, c and the time evolution of the values of H_1, p_{11}, T, and p at the wall in Table II. In contrast to the case of heating, sudden cooling gives rise to a pressure decrease near the wall, which causes a gas flow toward the wall and sends out an expansion wave. Owing to the gas flow, the density near the wall begins to increase. This leads to the pressure rise, and a compression wave is sent out. The compression wave overtakes the preceding expansion wave and weakens it. Only a small part of the disturbance in the temperature propagates as the expansion wave, and the rest diffuses slowly. In Fig. 8, we show the reduced velocity distribution function g at $t/t_0 = 0.5$, 2, and 10 for $T_1/T_0 = 0.5$.

The results for a small temperature drop, i.e., $T_1/T_0 = 0.9$, are shown in Fig. 9 and Table II, where some results of the linearized analysis[1] are also given. The pattern of the time development of the disturbance is very similar to that for $T_1/T_0 = 0.5$.

---

* Even in the case of $T_1/T_0 = 2$, the amplitude of the shock wave is small (see Fig. 4).

The lattice system used in the computation is as follows (the dimensionless variables x, $\bar{t}$, ζ are used below). The molecular velocity ζ is limited to the finite interval $-Z \leq \zeta \leq Z$ with $Z = 6$ ($T_1/T_0 < 1$) or 7 ($T_1/T_0 > 1$), which is divided into 120 nonuniform sections with the minimum width $2.68\times10^{-2} \sim 3.07\times10^{-2}$ around $\zeta = 0$ and the maximum width $0.305 \sim 0.373$ around $\zeta = \pm Z$. The space coordinate x is limited to the finite interval $0 \leq x \leq D$, where the subregion $0 \leq x \leq D_1$ ($D_1 \cong 21$) is divided into N_1 nonuniform sections with the minimum width Δ_m around $x = 0$ and the maximum width Δ_M around $x = D_1$, and the rest $D_1 \leq x \leq D$ is divided into N_2 uniform sections with the width Δ_M. For $0 \leq \bar{t} \leq 100$, $D \cong 21 \sim 133$, $N_1 = 1500 \sim 375$, $N_2 = 0 \sim 1125$, $\Delta_m = 0.0025 \sim 0.01$, and $\Delta_M = 0.025 \sim 0.1$; for $100 < \bar{t} \leq 2000$, $D \cong 283 \sim 2383$, $N_1 = 188 \sim 24$, $N_2 = 1312 \sim 1476$, $\Delta_m = 0.02 \sim 0.16$, and $\Delta_M = 0.2 \sim 1.6$; and for $2000 < \bar{t} \leq 10000$, $D \cong 15983$, $N_1 = 24$, $N_2 = 9976$, $\Delta_m = 0.16$, and $\Delta_M = 1.6$. The time step in $\bar{t}$ is changed, according as time, from the minimum step 0.0025 ($0 \leq \bar{t} \leq 100$) to the maximum step 0.1 ($2000 < \bar{t} \leq 10000$).

Let us denote the lattice system described above by $L1$. For an accuracy test, we prepared two coarser lattice systems $L2$ and $L3$, i.e., $L1$ with double the time step intervals ($L2$) and $L1$ with double the space lattice intervals ($L3$), and carried out the computation until $\bar{t} = 100$. To show the data, we introduce

$$S(x,\bar{t}) = \max(|M(L1) - M(L2)|, |M(L1) - M(L3)|),$$

(for each lattice point in $(x,\bar{t})$ common to $L1$,$L2$,and $L3$),

$$\bar{S}(\bar{t}) = \max_{0\leq x<\infty} S(x,\bar{t}),$$

where M represents the macroscopic variables $T_0^{-1}T$, $p_0^{-1}p$, etc. and $M(L1)$, etc. indicate the M computed on the basis of lattice $L1$, etc. Then, $S(0,\bar{t})$ for $p_0^{-1}(2RT_0)^{-1/2}H_1$, $p_0^{-1}p_{11}$, $T_0^{-1}T$, and $p_0^{-1}p$ are, respectively, less than the following (cf. Tables I and II):

3.0×10^{-4}, 1.8×10^{-4}, 3.7×10^{-4}, and 3.2×10^{-4}, ($T_1/T_0 = 2$),
3.1×10^{-5}, 1.4×10^{-5}, 3.0×10^{-5}, and 1.7×10^{-5}, ($T_1/T_0 = 1.1$),
4.0×10^{-4}, 1.4×10^{-4}, 3.0×10^{-4}, and 1.9×10^{-4}, ($T_1/T_0 = 0.5$),
3.2×10^{-5}, 1.5×10^{-5}, 3.0×10^{-5}, and 1.9×10^{-5}, ($T_1/T_0 = 0.9$),

$0.1 \leq \bar{t} \leq 100.$

$\bar{S}(10m)$ $(m = 1, 2, \cdots, 10)$ for $T_0^{-1}T$, $p_0^{-1}p$, and $(2RT_0)^{-1/2}v_1$ are, respectively, less than the following:

1.4×10^{-3}, 2.0×10^{-3}, and 9.9×10^{-4}, ($T_1/T_0 = 2$),
5.9×10^{-5}, 1.1×10^{-4}, and 6.1×10^{-5}, ($T_1/T_0 = 1.1$),
9.0×10^{-4}, 8.8×10^{-4}, and 5.2×10^{-4}, ($T_1/T_0 = 0.5$),
5.8×10^{-5}, 1.1×10^{-4}, and 6.1×10^{-5}, ($T_1/T_0 = 0.9$).

REFERENCES

1. Y. Sone, J. Phys. Soc. Jpn. **20**, 222 (1965).
2. A. A. Kovitz and K. H. Hellman, in Rarefied Gas Dynamics, edited by D. Dini (Editrice Tecnico Scientifica, Pisa, 1971), p. 811.
3. Y. Sone, K. Aoki, and I. Yamashita, in Rarefied Gas Dynamics, edited by V. C. Boffi and C. Cercignani (Teubner, Stuttgart, 1986), Vol. 2, p. 323.
4. Y. Sone and H. Sugimoto, J. Vac. Soc. Jpn. **31**, 420 (1988) (in Japanese).
5. K. Aoki, Y. Sone, and T. Yamada, Phys. Fluids A (to be published).
6. H. Sugimoto and Y. Sone, J. Vac. Soc. Jpn. **32**, 214 (1989) (in Japanese).
7. Y. Sone and H. Sugimoto, in Adiabatic Waves in Liquid-Vapor Systems, edited by G. E. A. Meier and P. A. Thompson (Springer, Berlin, 1990), p. 293.
8. C. K. Chu, Phys. Fluids **8**, 12 (1965).
9. H. Sugimoto, master's thesis, Kyoto University (1989) (in Japanese).
10. Y. Sone and Y. Onishi, J. Phys. Soc. Jpn. **44**, 1981 (1978).

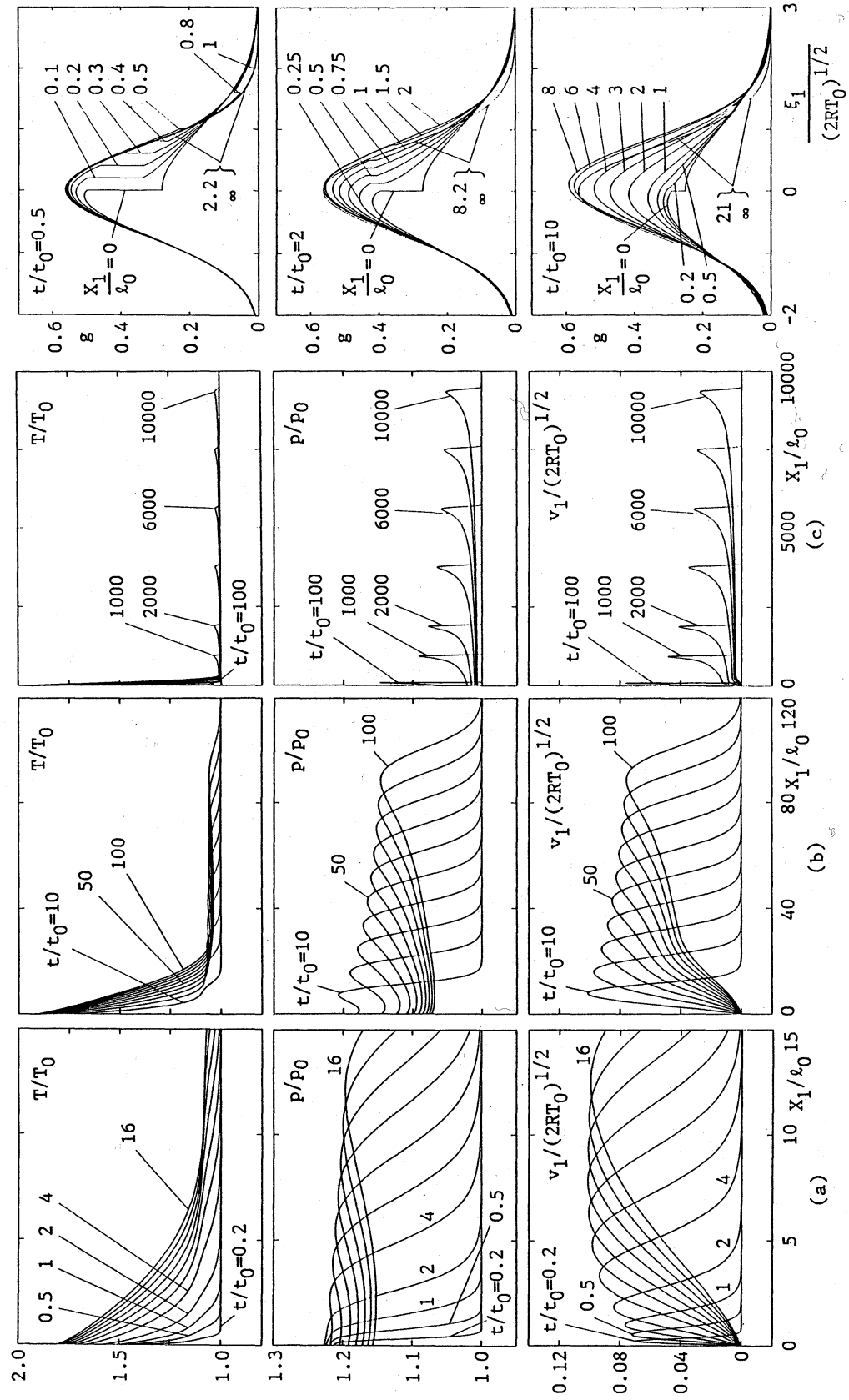

Fig. 4. The time development of the profiles of T, p, and v_1 for $T_1/T_0 = 2$.
(a) $t/t_0 = 0.2, 0.5, 1, 2m$ $(m = 1, 2, \cdots, 8)$, (b) $t/t_0 = 10m$ $(m = 1, 2, \cdots, 10)$,
(c) $t/t_0 = 100, 1000, 2000m$ $(m = 1, 2, \cdots, 5)$.

Fig. 5. The reduced velocity distribution function g for $T_1/T_0 = 2$.

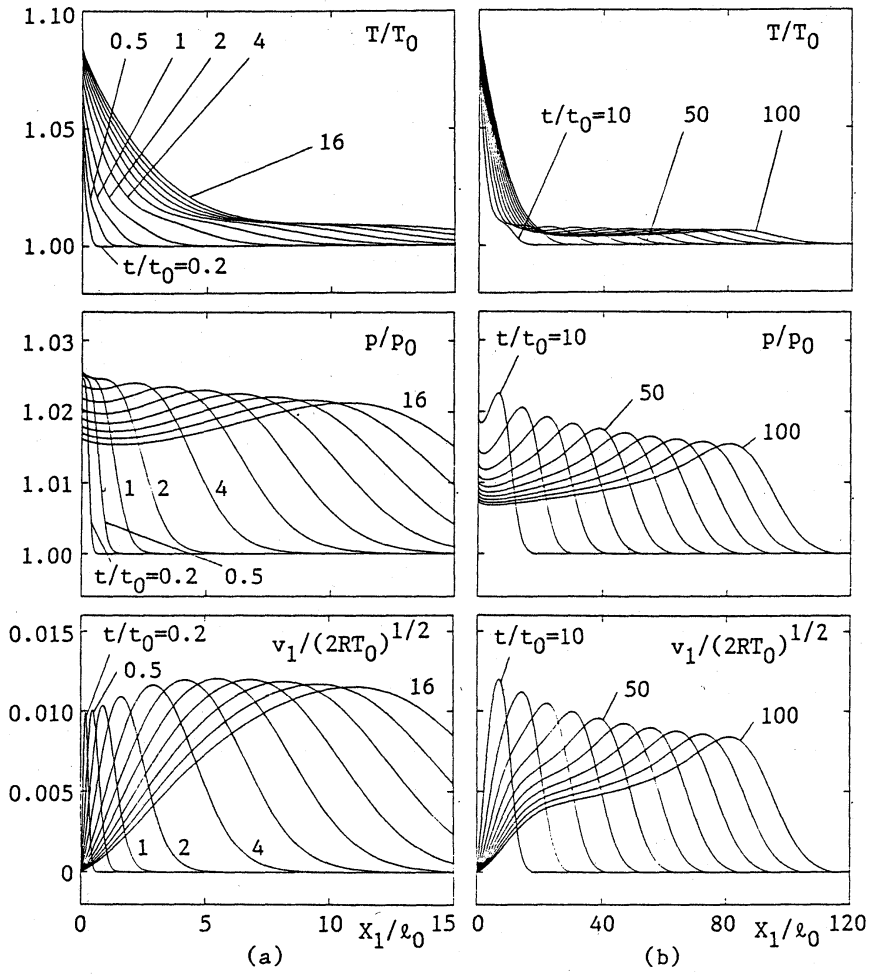

Fig. 6. The time development of the profiles of T, p, and v_1 for $T_1/T_0 = 1.1$. (a)$t/t_0 = 0.2, 0.5, 1, 2m$ $(m = 1, 2, \cdots, 8)$, (b)$t/t_0 = 10m$ $(m = 1, 2, \cdots, 10)$.

	$\frac{t}{t_0}$	$\frac{H_1(0,t)}{p_0(2RT_0)^{1/2}}$	$\frac{p_{11}(0,t)}{p_0}$	$\frac{T(0,t)}{T_0}$	$\frac{p(0,t)}{p_0}$
[$T_1/T_0 = 2$]	0	0.5642*	1.2071*	1.4142*	1.2071*
	0.1	0.5546	1.2076	1.4264	1.2096
	0.2	0.5453	1.2081	1.4382	1.2119
	0.5	0.5198	1.2090	1.4704	1.2175
	1	0.4833	1.2089	1.5157	1.2232
	2	0.4273	1.2055	1.5830	1.2259
	4	0.3555	1.1938	1.6639	1.2170
	6	0.3113	1.1817	1.7101	1.2038
	8	0.2808	1.1711	1.7403	1.1914
	10	0.2582	1.1619	1.7621	1.1805
	15	0.2200	1.1442	1.7978	1.1596
	20	0.1953	1.1316	1.8204	1.1449
	40	0.1438	1.1002	1.8669	1.1094
	100	0.0930	1.0666	1.9129	1.0723
	200	0.0664	1.0480	1.9374	1.0519
	500	0.0421	1.0306	1.9600	1.0331
	1000	0.0298	1.0217	1.9716	1.0234
	2000	0.0210	1.0154	1.9799	1.0166
	5000	0.0133	1.0097	1.9873	1.0105
	10000	0.0094	1.0069	1.9910	1.0074
[$T_1/T_0 = 1.1$]	0	0.0564*	1.0244*	1.0488* (1.0500)*	1.0244* (1.0250)*
	0.1	0.0554	1.0243	1.0501 (1.0514)	1.0246 (1.0252)
	0.2	0.0544	1.0243	1.0513 (1.0527)	1.0248 (1.0254)
	0.5	0.0516	1.0240	1.0547 (1.0568)	1.0252 (1.0261)
	1	0.0477	1.0236	1.0592	1.0255
	2	0.0419	1.0227	1.0656	1.0253
	4	0.0348	1.0208	1.0728	1.0236
	6	0.0304	1.0192	1.0767	1.0219
	8	0.0275	1.0179	1.0793	1.0203
	10	0.0253	1.0168	1.0811 (1.0797)	1.0191 (1.0241)
	15	0.0215	1.0148	1.0841 (1.0834)	1.0166 (1.0197)
	20	0.0191	1.0133	1.0860 (1.0857)	1.0149 (1.0170)
	30	0.0160	1.0113	1.0883 (1.0883)	1.0126 (1.0139)
	40	0.0141	1.0100	1.0898 (1.0899)	1.0112 (1.0120)
	60	0.0117	1.0084	1.0916 (1.0917)	1.0093 (1.0098)
	100	0.0092	1.0066	1.0934 (1.0936)	1.0074 (1.0076)

Table I. The time evolution of the physical quantities H_1, p_{11}, etc. at the wall for $T_1/T_0 = 2$ and 1.1. The values in the parentheses are the analytical results[1] for short and long times based on the linearized equation, and * indicates the exact values as $t/t_0 \to 0$ (The small difference between the limiting values inside and outside the parentheses is due to the nonlinearity).

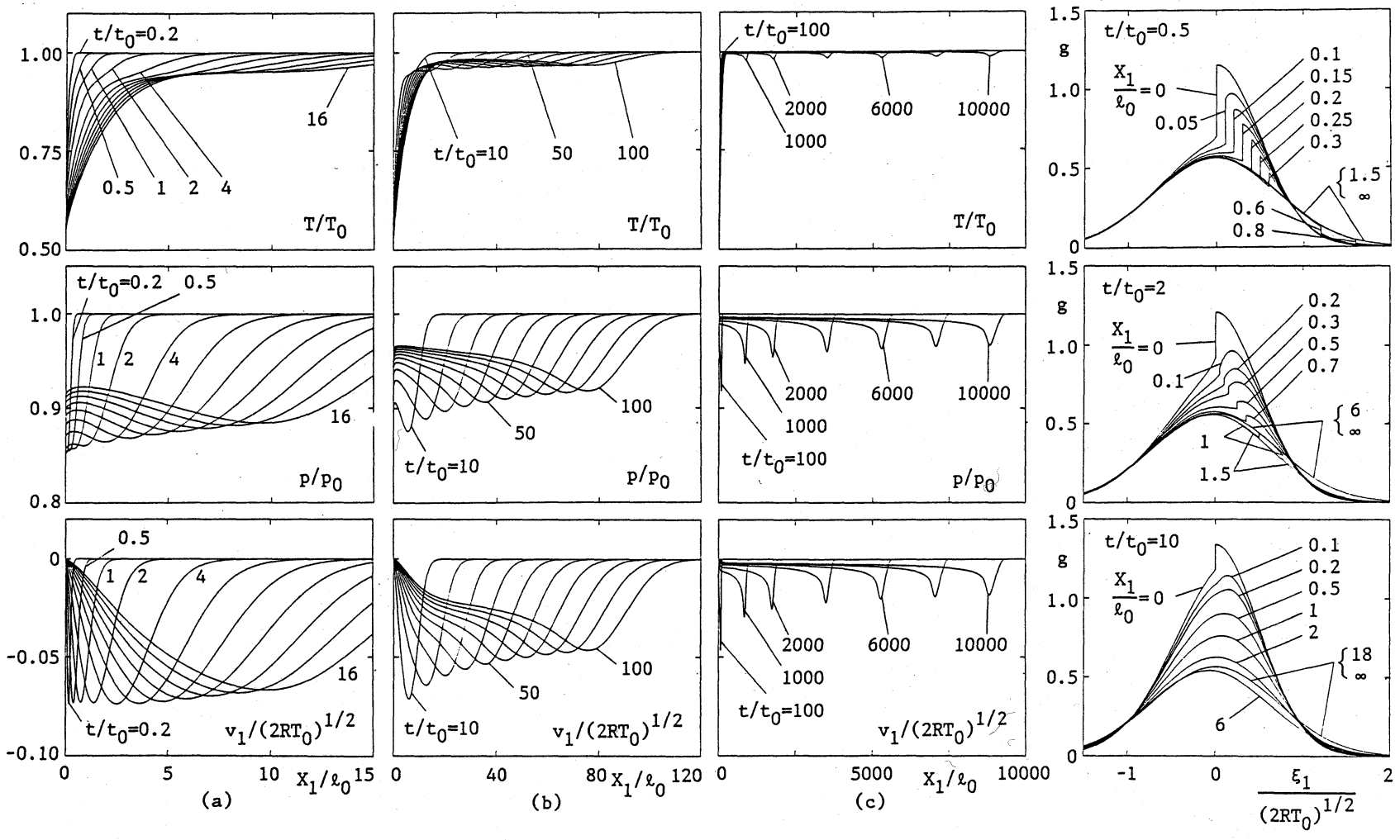

Fig. 7. The time development of the profiles of T, p, and v_1 for $T_1/T_0 = 0.5$. (a) $t/t_0 = 0.2, 0.5, 1, 2m$ $(m = 1, 2, \cdots, 8)$, (b) $t/t_0 = 10m$ $(m = 1, 2, \cdots, 10)$, (c) $t/t_0 = 100, 1000, 2000m$ $(m = 1, 2, \cdots, 5)$.

Fig. 8. The reduced velocity distribution function g for $T_1/T_0 = 0.5$.

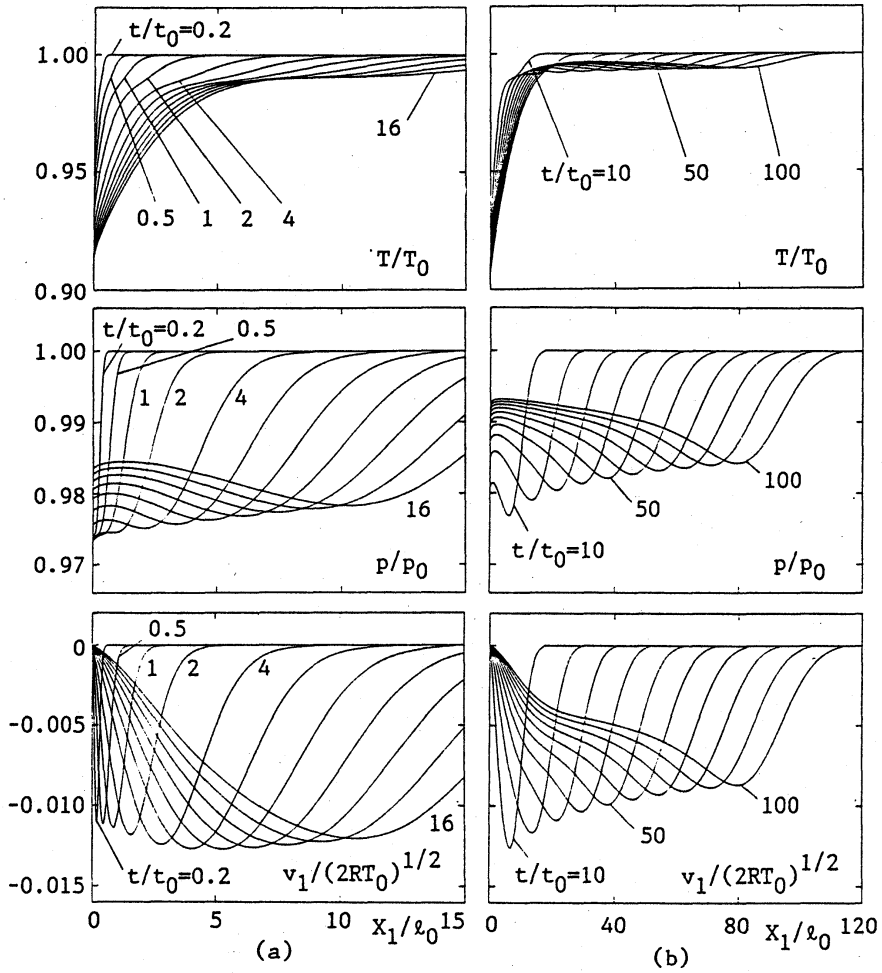

Fig. 9. The time development of the profiles of T, p, and v_1 for $T_1/T_0 = 0.9$. (a) $t/t_0 = 0.2, 0.5, 1, 2m$ $(m = 1, 2, \cdots, 8)$, (b) $t/t_0 = 10m$ $(m = 1, 2, \cdots, 10)$.

	$\frac{t}{t_0}$	$\frac{H_1(0,t)}{p_0(2RT_0)^{1/2}}$	$\frac{p_{11}(0,t)}{p_0}$	$\frac{T(0,t)}{T_0}$	$\frac{p(0,t)}{p_0}$
[$T_1/T_0 = 0.5$]	0	-0.2821*	0.8536*	0.7071*	0.8536*
	0.1	-0.2766	0.8548	0.7001	0.8529
	0.2	-0.2714	0.8560	0.6936	0.8524
	0.5	-0.2573	0.8594	0.6768	0.8517
	1	-0.2376	0.8648	0.6552	0.8523
	2	-0.2084	0.8741	0.6270	0.8572
	4	-0.1727	0.8884	0.5978	0.8706
	6	-0.1513	0.8989	0.5825	0.8825
	8	-0.1366	0.9069	0.5729	0.8921
	10	-0.1257	0.9133	0.5660	0.8998
	15	-0.1069	0.9250	0.5549	0.9136
	20	-0.0948	0.9328	0.5480	0.9227
	40	-0.0699	0.9497	0.5347	0.9422
	100	-0.0456	0.9669	0.5223	0.9619
	200	-0.0326	0.9763	0.5159	0.9726
	500	-0.0206	0.9850	0.5100	0.9827
	1000	-0.0144	0.9895	0.5069	0.9879
	2000	-0.0102	0.9926	0.5049	0.9914
	5000	-0.0064	0.9953	0.5031	0.9946
	10000	-0.0045	0.9967	0.5022	0.9962
[$T_1/T_0 = 0.9$]	0	-0.0564*	0.9743*	0.9487* (0.9500)*	0.9743* (0.9750)*
	0.1	-0.0554	0.9745	0.9474 (0.9487)	0.9742 (0.9748)
	0.2	-0.0543	0.9746	0.9461 (0.9473)	0.9740 (0.9746)
	0.5	-0.0515	0.9749	0.9428 (0.9432)	0.9737 (0.9740)
	1	-0.0476	0.9755	0.9383	0.9735
	2	-0.0418	0.9767	0.9321	0.9739
	4	-0.0346	0.9788	0.9252	0.9757
	6	-0.0303	0.9805	0.9214	0.9777
	8	-0.0274	0.9819	0.9190	0.9793
	10	-0.0252	0.9830	0.9173 (0.9203)	0.9807 (0.9759)
	15	-0.0215	0.9852	0.9145 (0.9166)	0.9832 (0.9803)
	20	-0.0190	0.9867	0.9128 (0.9143)	0.9850 (0.9830)
	30	-0.0160	0.9887	0.9106 (0.9117)	0.9873 (0.9861)
	40	-0.0141	0.9900	0.9093 (0.9101)	0.9888 (0.9880)
	60	-0.0117	0.9916	0.9077 (0.9083)	0.9906 (0.9902)
	100	-0.0092	0.9934	0.9060 (0.9064)	0.9926 (0.9924)

Table II. The time evolution of the physical quantities H_1, p_{11}, etc. at the wall for $T_1/T_0 = 0.5$ and 0.9. The values in the parentheses are the analytical results[1] for short and long times based on the linearized equation, and * indicates the exact values as $t/t_0 \to 0$ (The small difference between the limiting values inside and outside the parentheses is due to the nonlinearity).